RAPID COMMUNICATIONS

PHYSICAL REVIEW B

CONDENSED MATTER

THIRD SERIES, VOLUME 52, NUMBER 20 15 NOVEMBER 1995-II

## RAPID COMMUNICATIONS

*Rapid Communications are intended for the accelerated publication of important new results and are therefore given priority treatment both in the editorial office and in production. A Rapid Communication in* **Physical Review B** *may be no longer than four printed pages and must be accompanied by an abstract. Page proofs are sent to authors.*

# Influence of charge and magnetic ordering on the insulator-metal transition in $Pr_{1-x}Ca_xMnO_3$

M. R. Lees, J. Barratt, G. Balakrishnan, and D. McK. Paul
*Physics Department, University of Warwick, Coventry CV4 7AL, United Kingdom*

M. Yethiraj
*Solid State Division, Oak Ridge National Laboratory, Oak Ridge, Tennessee 37831-6393*
(Received 18 August 1995)

A detailed study of the properties of $Pr_{1-x}Ca_xMnO_3$ shows that for a range of compositions ($0.3 \leq x < 0.5$) there is a first-order magnetic-field-induced insulator-metal transition. For the $x = 0.4$ composition the magnetic and charge ordering (CO) effects are decoupled with antiferromagnetic (AFM) ordering, $T_N = 170$ K, developing at considerably lower temperatures than the CO state, $T_{CO} = 250$ K. Below the CO temperature, metamagnetic transitions exist that transform the magnetic correlations from either paramagnetic or AFM to ferromagnetic. Metastable conducting states are formed below 25 K.

Large negative magnetoresistance (MR) is of current interest due to the possibility of producing devices which make use of this effect. This property can be tailored by making thin films consisting of various layers,[1,2] but is also found to occur naturally in doped manganite compounds. The substitution of divalent ions on the rare-earth ($R$) site in $RMnO_3$ compounds yields materials for which the application of a magnetic field produces very large decreases in resistivity.[3–5] Additional large changes in resistivity occur when these compounds magnetically or charge order.[5–9] These effects are due primarily to the effective increase in the Mn valence created by the doping. As the doping increases it becomes easier for an outer electron to hop between Mn ions creating a tendency for ferromagnetic (FM) interactions rather than the antiferromagnetic (AFM) exchange interactions which dominate if this electron is localized. Such effects have been discussed in terms of the double exchange interaction which simply describes the dominance of the different interactions on doping.[10–12] However, recent numerical estimates of the role of this interaction have shown that it is incompatible with the experimental observations and suggests that a polaron picture would be a better model for the dominant interactions.[13] It is also possible to order the Mn ions into a $Mn^{3+}/Mn^{4+}$ sublattice [charge ordering (CO)] at compositions near 50% doping.[9] This creates a large increase in resistivity, again due to the restriction on the mobility of the electrons and the formation of an AFM ground state. Application of a magnetic field can melt this CO state leading to a large decrease in resistivity and a FM state. The electronic structure in such materials is also strongly coupled to the lattice structure and it has been shown that, in certain cases, it is possible to force a structural phase transition at constant temperature by the application of a magnetic field.[14]

The clearest example of the influence of CO is observed in studies of $Pr_{0.5}Sr_{0.5}MnO_3$.[9] This material has a FM transition at 270 K, below which there is a matching change in the magnetization and the resistivity. At 140 K charge ordering occurs with a simultaneous transition into an AFM state and a large increase in resistivity due to the localization of the charge carriers. Below the CO/AFM transition temperature, the FM/conducting state can be retrieved by applying a sufficiently large external magnetic field. A magnetic field of 62 kOe is required to melt the CO lattice at low temperatures ($T < 50$ K). A degree of hysteresis accompanies this transition, suggesting that the phase transition is first order. These effects are very dependent on composition in this material and are restricted to a small range of composition around 50% doping.

The substitution of Ca for Pr in $PrMnO_3$ shows the influence of CO but the flexibility of the perovskite lattice and the smaller divalent ion allows charge ordering to persist, albeit

 

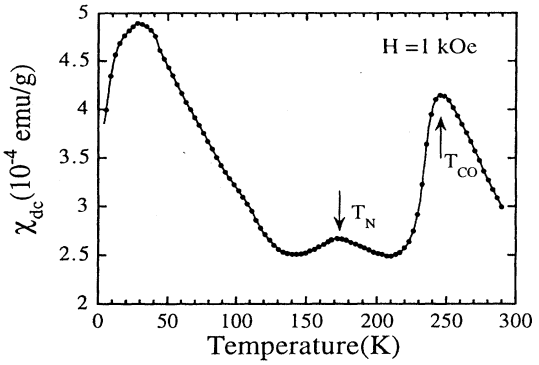


FIG. 1. $\chi_{dc}$-$T$ for $Pr_{0.6}Ca_{0.4}MnO_3$. The sample was zero field cooled and the data collected in an applied field of 1 kOe.

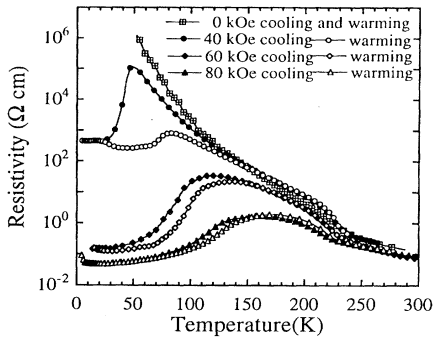


FIG. 2. $\rho$-$T$ for $Pr_{0.6}Ca_{0.4}MnO_3$ taken in several magnetic fields. $\rho$ was measured while cooling the sample from 300 K under magnetic field and then during field-cooled warming.

in a disordered or locally clustered form, for 30% to 70% doping.[15] In this paper we shall present magnetization $M$, magnetic susceptibility $\chi$, resistivity $\rho$, and neutron scattering measurements on $Pr_{1-x}Ca_xMnO_3$, which demonstrate that much larger changes in resistivity exist in the disordered charge lattice system for 30% and 40% doping accompanied by extensive regions of hysteresis extending over a considerable range of temperature and magnetic field. Metastable states are formed below 25 K which produce extremely long time constants for the increase in $\rho$ on removal of the magnetic field. The magnetic and CO effects are decoupled in these compounds with, for example, the ordered AFM state ($T_N$=170 K) developing at considerably lower temperatures than the charge ordering ($T_{CO}$=250 K). For all temperatures below the CO temperature, metamagnetic transitions exist which transform the magnetic correlations from either paramagnetic or AFM into a FM system with the application of an external magnetic field.

$Pr_{1-x}Ca_xMnO_3$ forms across the whole composition range. As a consequence of a number of sources of distortion present in this system, including a buckling of the $MnO_6$ octahedra and a Jahn-Teller effect, $Pr_{1-x}Ca_xMnO_3$ assumes a variety of structures at different temperatures. This system also has a complex magnetic phase diagram.[15–17] Polycrystalline samples of $Pr_{1-x}Ca_xMnO_3$ ($0 \leq x \leq 1$) were prepared in air by reacting stoichiometric quantities of $Pr_6O_{11}$, $CaCO_3$, and $MnO_2$. Single crystals were melt grown in air by a floating-zone technique using an infrared image furnace. X-ray spectra of the samples showed them to be nominally single phase. The resistivity, magnetization, and susceptibility data presented here are for ceramic samples.

Figure 1 shows the temperature dependence of dc magnetic susceptibility for $x$=0.4. Curves of $\chi_{ac}$-$T$ are similar. Both contain a broad peak at around 250 K. A maximum in the $\chi$-$T$ data at 250 K is also seen for up to $x$=0.7, while there are no obvious features in the data above 200 K for $0.0 < x \leq 0.3$. $\rho$-$T$ measurements show that the resistivity is thermally activated for all values of $x$. Figure 2 contains data for the $x$=0.4 compound. A fit to a simple exponential dependence shows that the activation energy at high temperature decreases from 0.2 eV at $x$=0.0 to 0.07 eV at $x$=0.5. For $x \leq 0.2$ a single value for the activation energy is observed over the entire temperature range examined. For $0.3 < x \leq 0.7$ a change in the slope of $\rho$-$T$ around 250 K corresponds to an increase in the activation energy below this temperature. These features in the $\chi$ and $\rho$ data at 250 K are associated with CO and an orthorhombic to tetragonal structural transition, which occurs at this temperature for a wide composition range ($0.3 < x \leq 0.7$).[16] A second maximum in $\chi$-$T$ at 170 K indicates the onset of AFM ordering. This agrees well with a previous report[17] which suggests that for $0.4 < x \leq 0.5$ the materials order with a canted AFM structure with a $T_N$ of ~170 K. Thus the charge ordering and AFM ordering occur at different temperatures.

In zero field the room temperature (RT) resistivity of $Pr_{1-x}Ca_xMnO_3$ decreases from ~800 Ω cm for $x$=0.0 to ~0.003 Ω cm at $x$=0.5. The application of a magnetic field produces a decrease in $\rho$ which corresponds to a significant negative MR over a wide temperature and composition range. For a limited range of $x$ (0.3–0.4) the resistivity in field becomes metallic at low temperature (Fig. 2). For the $x$=0.4 composition, a peak in $\rho$-$T$ at 70 K in $H$=40 kOe is followed by a fall in $\rho$ at lower temperatures. As $H$ is increased, the position of this peak is shifted to a higher temperature and the magnitude of $\rho$ falls. At 4 K, $\rho$ can be varied by at least eight orders of magnitude depending on the value of the applied field. On warming from low temperature in fields above 60 kOe, there is a further decrease in $\rho$-$T$ producing a minimum around 40 K. The cooling and warming curves show hysteresis in the data with a width of up to 100 K. Similar behavior is observed for the $x$=0.3 sample. The field required to induce the low-temperature fall in $\rho$ is also around 40 kOe and the hysteresis is again large.

Figure 3 shows $\rho$-$H$ at fixed temperature for the $x$=0.4 sample. For each loop the sample was first zero field cooled (ZFC) from RT to the measuring temperature. At 4 K, $\rho$ is initially above the limit which we can measure. As the magnetic field is increased there is a rapid fall in $\rho$-$H$ around 50 kOe. $\rho$ falls by more than six orders of magnitude within 5 kOe. A more gradual decrease in $\rho$-$H$ by another two orders of magnitude is observed up to 80 kOe. Sweeping the field back to zero produces only a small increase in the magnitude of the resistivity. For higher temperatures the initial value of $\rho$ decreases in line with the $\rho$-$T$ data. At 45 K the transition to the conducting state occurs around 40 kOe and is more rounded. On decreasing the magnetic field the sample returns to an insulating state. At higher temperatures $\rho$ falls with increasing magnetic field, corresponding to a large negative MR. The $\rho$-$H$ loops open up only for higher fields with a very small hysteresis in zero field and there are no discontinuities in the data.

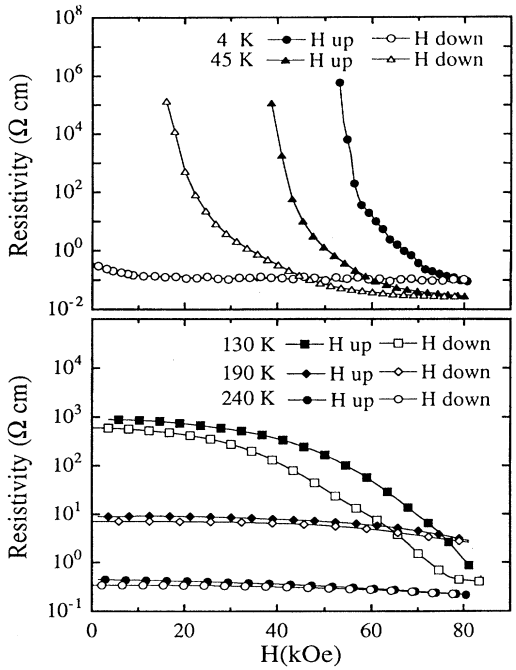


FIG. 3. $\rho$-$H$ data for $Pr_{0.6}Ca_{0.4}MnO_3$ taken at several temperatures. The measurements were performed after cooling the sample from 300 K in zero magnetic field.

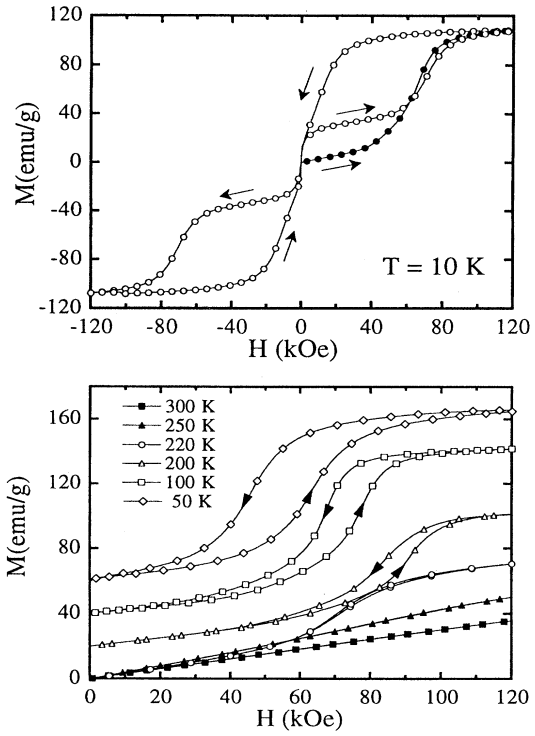


FIG. 4. Magnetization for $Pr_{0.6}Ca_{0.4}MnO_3$ taken at several temperatures as a function of magnetic field. The measurements were performed after cooling the sample from 300 K in zero magnetic field. The upper panel shows a full five quadrant hysteresis loop at 10 K. The closed symbols indicate the data collected during the initial field sweep. The lower panel shows data collected above (closed symbols) and below (open symbols) the charge-ordering temperature. Data taken below 220 K are offset for clarity.

Magnetization measurements reveal significant changes in magnetic ordering with increasing magnetic field. $M$-$H$ loops taken on a ZFC $x=0.4$ sample are shown in Fig. 4. The initial susceptibility agrees well with $\chi$-$T$ data and is characteristic of an AFM ordered state. A metamagnetic transition to FM ordering is observed at 50 kOe. The saturation moment corresponds to $3.95\mu_B$ per formula unit. This is slightly higher than the mean spin only value for Mn ions and may be explained by a small contribution from the Pr ions. Following the initial field sweep the $M$-$H$ loops trace out a symmetric path about the origin with an enhanced susceptibility at low fields. A rapid increase (decrease) in the magnitude of the signal at around 50 kOe (20 kOe) indicates the continuing presence of a metamagnetic transition from AFM to FM ordering. There is little or no remanence and a very small coercive field. The metamagnetic transition is shifted to higher field with increasing temperature and together with the irreversible behavior is present up to 250 K, the temperature of the CO transition.

There is a clear correlation between the magnetic state and the resistivity of the material. At 10 K, the field at which the metamagnetic transition occurs agrees well with the field at which the jump to a conducting state is observed. However, as the temperature is increased the appearance of the low resistivity state is observed at lower field values, while the metamagnetic transition in the $M$-$H$ data shifts to higher fields. The low temperature $M$-$H$ loops show that the initial field sweep produces an irreversible change in the magnetic state of the material. The low-temperature $\rho$-$H$ loops also indicate the appearance of a metastable conducting state. After application of an 80-kOe field, which for $x=0.4$ produces a $10^8$ decrease in $\rho$, subsequent relaxation measurements in zero field have shown that at 10 K, $\rho$ only doubles in 2 h. Relaxation rates increase rapidly with temperature and $\rho$ can be returned to its original value by annealing above 30 K. This temperature coincides with the low-temperature peak in the $\chi$ data. The conducting state is much more stable in samples with $x=0.3$ where the material must be annealed at much higher temperatures ($T>150$ K) in order to recover the insulating state.[18] In contrast, we have found that for a single crystal of the $x=0.4$ material it is not possible to stabilize a conducting state in zero field after field cycling, even at 4 K, with an abrupt return to the insulating state being observed as the field is reduced below 20 kOe.

Neutron diffraction experiments with a powdered sample of $Pr_{0.6}Ca_{0.4}MnO_3$ manufactured from a melt-processed rod containing a few crystallites confirm the findings of the magnetic and transport measurements. Magnetization, magnetic susceptibility, and specific-heat studies showed identical features for crystals from this rod and ceramic specimens. At all temperatures and fields the nuclear data were consistent with an orthorhombic symmetry of $Pbnm$. CO was observed below 250 K by the appearance of an additional Bragg contribution [a shoulder on the much stronger triplet (200),(020),(112) reflection] which could be approximately indexed as $(2\ \frac{1}{2}\ 2)$ and $(2\ \frac{3}{2}\ 0)$. These are the strongest estimated reflections from the proposed charge-ordered state. This contribution increased in intensity as the temperature was lowered. Additional Bragg reflections appeared below 160 K. These peaks could all be indexed as $h$ half integer, $k$ half integer or integer, and $l$ zero. These reflections are con-

sistent with an AFM arrangement of the spins with at least doubling of the nuclear cell in the $a$ and $b$ directions. Below ~30 K these reflections decreased in intensity and additional reflections appeared which corresponded to the same indexing but with $l$ integer but greater than zero. This transition correlates well with the peak observed in the susceptibility and can be well described by a spin reorientation with the direction of the Mn spins moving out of the $a$-$b$ plane to produce a component along the $c$ axis. It is possible that this spin reorientation transition is influenced by a tendency to order the Pr ions. When a magnetic field is applied at 4.2 K the AFM peaks disappear at ~50 kOe and there is a large increase in the intensity of the nuclear reflections at low angle. The metamagnetic transition therefore corresponds to a transition between an AFM and a FM state with the large decrease in resistivity being associated with change in magnetic ordering. On removing the magnetic field the system does not recover the ZFC magnetic state, but the strongest AFM peak can just be observed above background. The low-angle nuclear peaks which clearly demonstrated the ferromagnetic state in an applied field decrease markedly in intensity but do not return to their ZFC state. It is possible that this effect is due to a realignment of the sample under the influence of shape demagnetization or anisotropic susceptibility but could also be due to a structural change in an applied field and sufficient hysteresis to maintain the high-field structure after removing the field.[14] Further powder and single-crystal studies are currently underway to determine more effectively the changes produced by an applied field.

The results in this paper show that for $Pr_{1-x}Ca_xMnO_3$ there are a range of compositions ($0.3 \leq x < 0.5$) for which there is a first-order magnetic-field-induced transition from an insulating to a conducting state. For lower levels of Ca doping the activation energies are high. For the ordered composition $x=0.5$, magnetization and resistivity measurements reveal that the AFM and the CO states are stable and if the CO can be destroyed by a magnetic field then a field $H>120$ kOe is required.[19] For a range of values of $x$ around 0.4 there is a significant decrease in the activation energy and the AFM state is not fully established. For example, for $x=0.3$, magnetization and susceptibility data indicate that AFM and FM order appear to coexist with $T_N$ and $T_c$ of 130 and 115 K, respectively. Application of a magnetic field leads to breakdown of the CO state. The appearance of the conducting state is different in several ways from that observed in $Pr_{0.5}Sr_{0.5}MnO_3$. In zero field, $Pr_{1-x}Ca_xMnO_3$ shows activated behavior from 300 to 4 K and is never metallic. As a result, the changes in $\rho$ are orders of magnitude larger in this case. The conducting state in $Pr_{1-x}Ca_xMnO_3$ is metastable. In the case of $Pr_{0.5}Sr_{0.5}MnO_3$ there is some hysteresis associated with the first-order metamagnetic transition, but the system always returns to the insulating state as the field is reduced to zero. The role of disorder is obviously very important in this material with a bond percolation mechanism probably determining the magnetic properties and clustering influencing the actual state adopted under any given set of experimental conditions and the time constants for various metastable states. Various frustration mechanisms also may influence both the Pr and Mn magnetic configurations. Such contributions are best illustrated by the large hysteresis evident in the resistivity data and the difference between single-crystal and ceramic data. Grain boundaries and other defects could influence considerably the growth of domains and magnetic order by blocking the diffusion of the charge carriers when an applied field is removed and leaving extensive regions of metastable FM interactions which can only be annealed from the sample on a long time scale.

Perhaps the most important observation for the $x=0.3$–$0.4$ samples is the decoupling of the influence of CO from the onset of long-range magnetic order. In these materials the CO is clearly indicated by an increase in $\rho$ and a magnetic anomaly but the CO state formed may be sufficiently disordered that long-range magnetic order can only occur at lower temperatures. We would expect single-crystal experiments to show a degree of short-range AFM order between the CO and the AFM transition. In this region it is still possible to produce a FM state by the application of a magnetic field which is reflected in the electronic properties by a large negative MR. The field required for this transition from short-range AFM order to FM order is larger than that required to drive the system from long-range AFM to FM order at lower temperatures. The required field decreases with decreasing temperature. Lattice effects may also be important in determining these high-temperature anomalies. The large hysteresis which is associated with the low-temperature properties ($T<25$ K) appears in part to be coupled to the presence of a Pr moment which attempts, at least initially, to follow the local orientation of the Mn moments. Evidence for the presence of a Pr moment is provided by the estimated effective moment from magnetization studies. The coupling between Pr and Mn moments may drive the spin reorientation which is observed around this temperature and help create the metastable states which occur when an applied magnetic field is removed.

We are grateful to Dr. D. T. Adroja and C. D. Dewhurst for their help with the magnetization measurements. This research was supported in part by U.S. DOE, Contract No. DE-AC05-84OR21400 with Lockheed-Martin.

[1] M. N. Baibich, J. M. Broto, A. Fert, F. Nguyen Van Dau, F. Petroff, P. Etienne, G. Creuzet, A. Friederich, and J. Chazelas, Phys. Rev. Lett. **61**, 2472 (1988).

[2] S. S. P. Parkin, N. More, and K. P. Roche, Phys. Rev. Lett. **64**, 2304 (1990).

[3] S. Jin, T. H. Tiefel, M. McCormack, R. A. Fastncht, R. Ramesh, and L. H. Chen, Science **264**, 413 (1994).

[4] R. von Helmholt, J. Wecker, B. Holzapfel, L. Shultz, and K. Samwer, Phys. Rev. Lett. **71**, 2331 (1993).

[5] Y. Tokura, A. Urushibara, Y. Moritomo, T. Arima, A. Asamitsu, and N. Furukawa, J. Phys. Soc. Jpn. **63**, 3931 (1994).

[6] G. H. Jonker and J. H. van Santen, Physica **16**, 337 (1950).

[7] E. O. Wollan and W. C. Koehler, Phys. Rev. **100**, 545 (1955).

[8] G. H. Jonker, Physica **22**, 707 (1956).

[9] Y. Tomioka, A. Asamitsu, Y. Moritomo, H. Kuwahara, and Y. Tokura, Phys. Rev. Lett. **74**, 5108 (1995).
[10] C. Zener, Phys. Rev. **82**, 403 (1951).
[11] P. W. Anderson and H. Hasegawa, Phys. Rev. **100**, 675 (1955).
[12] P.-G. de Gennes, Phys. Rev. **118**, 141 (1960).
[13] A. J. Mills, P. B. Littlewood, and B. I. Shraiman, Phys. Rev. Lett. **74**, 5144 (1995).
[14] A. Asamitsu, Y. Moritomo, Y. Tomioka, T. Arima, and Y. Tokura, Nature (London) **373**, 407 (1995).
[15] Z. Jirak, S. Vratislav, and J. Zajicek, Phys. Status Solidi **52**, K39 (1979).
[16] E. Pollert, S. Krupicka, and E. Kumzicova, J. Phys. Chem. Solids **43**, 1137 (1982).
[17] Z. Jirak, S. Krupicka, Z. Simsa, M. Dlouha, and S. Vratislav, J. Magn. Magn. Mater. **53**, 153 (1985).
[18] J. Barrat, M. R. Lees, G. Balakrishnan, and D. McK. Paul (unpublished).
[19] J. Barrat, M. R. Lees, G. Balakrishnan, and D. McK. Paul (unpublished).